

DEVELOPMENT OF HIGH VOLTAGE ELECTRIC PULSE CHARGING AND DISCHARGING DEVICE BASED ON FUNCTIONAL MATERIALS

Fang Zhou*

Fanli School of Business, Nanyang Institute of Technology, Nanyang, Henan,
473004, China

shangxy1921@163.com

Reception: 19/02/2023 **Acceptance:** 15/04/2023 **Publication:** 08/05/2023

Suggested citation:

Zhou, F. (2023). **Development of high voltage electric pulse charging and discharging device based on functional materials.** *3C TIC. Cuadernos de desarrollo aplicados a las TIC*, 12(2), 77-95. <https://doi.org/10.17993/3ctic.2023.122.77-95>

ABSTRACT

As a relatively mature energy storage technology, charge/discharge devices are bound to develop significantly in the contemporary society among them energy is increasingly scarce. The traditional charging and discharging device is not smart enough, slow charging and discharging and other shortcomings have limited its further high-speed development. The application of functional materials and high-voltage pulse technology can drive the further development of charging and discharging devices. In this study, a safe, low-cost, functional material with high adsorption capacity was developed. At the same time, this functional material is applied to the charging and discharging device to improve the storage capacity and discharge efficiency of the device. In addition, we combine high-voltage electric pulse technology with charging and discharging technology to improve the charging and discharging rate of the charging and discharging device. It has certain guidance and reference values for the development of high-voltage electric pulse charging and discharging devices. According to the test results, the dynamic adjustment time of the charging module output current is only 20ms, and the dynamic adjustment response time of the discharging module input current is about 0.14s. The device provides a new idea for the development of high-voltage electric pulse charging and discharging equipment.

KEYWORDS

Functional materials; high-voltage pulses; charging and discharging devices; system design; electrochemical perform

INDEX

ABSTRACT

KEYWORDS

1. INTRODUCTION

2. MATERIAL CHARACTERIZATION AND CHARGE/DISCHARGE SYSTEM DESIGN

2.1. Material property characterization test

2.1.1. X-ray diffraction analysis

2.1.2. Fourier transform infrared spectral analysis

2.1.3. Micromorphological analysis

2.1.4. Raman spectral analysis

2.2. Electrochemical performance testing

2.2.1. Cyclic voltammetry (CV)

2.2.2. Constant current charge/discharge method (GCD)

2.2.3. Electromagnetic Wave Absorption Performance test

2.3. Charging and discharging device system design

2.4. Factors affecting the life of charging and discharging devices

2.4.1. Charging voltage

2.4.2. Anti-peak voltage

2.4.3. Peak discharge current

2.4.4. Temperature

2.4.5. Other factors

3. RESULTS AND DISCUSSION

3.1. Charging process

3.2. Discharge process

3.3. Verification of charging and discharging functions

3.4. Dynamic adjustment of the input current of the discharge module

4. CONCLUSION

REFERENCES

1. INTRODUCTION

With the scarcity of fossil energy and the great development of renewable energy, the demand for energy storage in power systems is becoming more and more urgent^[1-3]. Charge discharge technology is widely used in electric power, railway transportation, automobile industry and marine industry. However, low efficiency, unfriendly environment and inconvenient operation limit the further development of charge and discharge technology to a certain extent^[4]. The rapid development of productivity and increasingly serious environmental problems force people to put forward higher requirements for the performance of charging and discharging devices, so there is an urgent need to design an efficient, intelligent and reversible charging device^[5-6].

Functional materials^[7] mainly refer to those with excellent electrical, magnetic, optical, thermal, acoustic, mechanical, chemical, biomedical functions and special physical, chemical, biological effects, which can complete the mutual transformation of functions. These high-tech materials are mainly used to manufacture various functional components and are widely used in various high-tech fields^[8-9]. With a wide variety of functional materials and a wide range of applications, a large-scale high-tech industry group is being formed, which has a very broad market prospect and extremely important strategic significance. All countries in the world attach great importance to the research, development and application of functional materials, which have become the hotspot and focus of new materials research and development in the world, as well as the hotspot of strategic competition in the development of high technology in the world^[10-11]. Lu et al^[12] developed a two-dimensional semiconductor functional material (CaP_3) with certain porosity and ultra-high carrier mobility. They found that this new functional material has a direct band gap of 1.15 eV and also has a very high electron mobility, which has great potential for applications in nanoelectronics. In addition to the above two characteristics, CaP_3 also exhibits good light absorption properties in the entire visible range. The innovative electronic and charge mobility as well as optical properties make such materials a potential army for future nanoelectronics and optoelectronics. xiao et al^[13] designed and fabricated a functional material with excellent electrocatalytic properties and applied it in electrochemistry. Multifunctional cobalt hydroxide decorated homogeneous porous hollow carbon spheres (CoOOH-PHCS) can act as electrocatalysts to suppress the shuttle effect in lithium-sulfur batteries on the one hand, and accelerate the rate of redox reactions on the other. Moreover, thanks to the coordinated effect of these two materials, CoOOH and PHCS, the electrode exhibited an ultra-low capacity decay of 0.04% per cycle over 450 cycles at 1C. Their work explores and reveals the potential of CoOOH for electrocatalytic applications. Li et al^[14] developed a CO_2 gas thermal conductivity sensor based on graphene oxide (GO) and $\alpha\text{-Al}_2\text{O}_3$ and calculated the stability of this sensor by simulation. The results show that this sensor has excellent gas heat exchange rate and good stability, and also exhibits good linearity and zero-point stability with CO_2 gas. They developed a CO_2 gas thermal conductivity sensor with shorter response and response times and

lower power consumption compared to conventional thermal conductivity sensors. Wang et al^[15] reviewed the recent research on photonic devices based on functional material infiltrated photonic crystal fibers (PCF). They pointed out that PCFs have a unique arrangement of stomata in their two-dimensional orientation, and these stomata provide natural optofluidic channels for introducing materials, enhancing optical matter interactions, and extending transmission properties. This unique photonic device is widely used for compact and multifunctional integration as well as electromagnetic resistance. Compagnone et al^[16] argued that although phytochemical products are starting to be widely used to assist in the exfoliation of 2D nanomaterials, there is a clear lack of research on the molecules involved and their ability to yield functional materials. They proposed a new green liquid phase exfoliation (LPE) strategy to analyze this, characterizing the morphological, structural and electrochemical properties of GF-CT by physicochemical and electrochemical methods. The results show that GF-CT exhibits good electrochemical properties without modification and also has high sensitivity at low overpotential.

High-voltage pulse technology is a technology with great development potential and also a key planning and development technology in China. Its products have high technical content, can provide very large peak currents, are advanced and highly reliable, and have a wide range of applications in the power industry, defense industry, and other high-tech fields^[17-19]. Rao et al^[20] used granite as an example to establish the electric pulse rock-breaking equivalent circuit, shock wave models in the electric channel plasma, and especially rock damage models. The results predicted from these models were used to analyze and reveal the rock destruction process under the action of high-voltage electrical pulses in order to evaluate and improve the efficiency of high-voltage pulse technology in geological drilling, tunneling, and other geotechnical applications. Dong et al^[21] used a bipolar high-voltage pulse dielectric blocking discharge method for denitrification of exhaust gas in order to improve the removal rate of nitrogen compounds from automobile exhaust gas and reduce the environmental impact of automobile exhaust gas. The results showed that the use of a threaded copper rod as the discharge electrode and quartz glass as the medium had a better denitrification effect. Li et al^[22] applied the high-voltage pulse technique to the field of hard rock construction drilling and breaking, and developed a prediction model for the discharge circuit based on Bayesian fusion. The results showed that this model reduced the average relative error by 25.5% compared with the traditional single model, which further improved the accuracy and reliability of the model prediction. Li et al^[23] proposed the application of high pressure pulse technology to the coal industry in order to solve the challenges of coal desulfurization and ash removal. They showed that high voltage pulses can selectively breakdown minerals with higher conductivity or dielectric constants than coal, which are then separated by size differences to remove sulfur- and ash-bearing minerals containing pyrite. The results showed that after a single high-voltage pulse discharge, more than 75% of the high-density particles were broken up, while the low-density particles could still remain intact, resulting in more efficient desulfurization and ash removal from coal.

In terms of charging and discharging devices, a reversible rectifier high-capacity charging and discharging power supply with SVPWM technology is necessary, characterized by an integrated charging and discharging main circuit that is both a charging circuit and a discharging inverter energy recovery circuit^[24-26]. This allows for compact equipment, improved device utilization, and pulsed charging and discharging functions along with conventional charging and discharging. With SVPWM technology, high power factor and high efficiency of the device are achieved, and harmonic components are greatly improved and reduced. In addition, the fuzzy double closed-loop control of voltage and current is used in the control, which can ensure the steady-state accuracy of charging and discharging with constant current and voltage control, as well as the good dynamic response performance of the device^[27-29]. Sodhi et al^[30] proposed a numerical model for a horizontal conical shell-and-tube energy storage device to investigate its charging and discharging characteristics. The numerical results show that the innovative design by replacing the circular shell with a conical shell leads to an increase in the heat transfer rate of the whole energy storage device. Also the installation of fins outside the tube affects the performance of the device. Jaewon et al^[31] proposed a fast charging system for wireless railroad trains using an input voltage sharing topology and a balanced control scheme. This system changes the traditional way of charging trains from roadside devices and uses on-board devices to store energy by fast charging during the train's inbound stop, which is convenient and efficient with a stable system. Choi et al^[32] analyzed the charge and discharge characteristics of a hybrid electric propulsion system. They proposed a hybrid power system in which the ship is propelled only by the electrical energy stored in the battery at low speeds, while water jet propulsion is used in other operating conditions. From the analysis results, it is clear that this hybrid power system can help the ship achieve efficient, zero-emission and silent navigation.

In summary, functional materials, high-voltage pulses, and charging and discharging devices have great potential in their respective fields, but there are few studies combining all three of them. In this study, we aim to develop a safe, low-cost and efficient adsorption material with high adsorption capacity and low desorption rate, and obtain a functional material with high adsorption capacity and low desorption rate. Meanwhile, this functional material is applied to charge/discharge devices to improve the storage capacity and discharge efficiency of the devices. In addition, it is proposed to combine high voltage pulse technology with charging and discharging technology to improve the charging and discharging rate of the charging and discharging device.

2. MATERIAL CHARACTERIZATION AND CHARGE/DISCHARGE SYSTEM DESIGN

2.1. MATERIAL PROPERTY CHARACTERIZATION TEST

2.1.1. X-RAY DIFFRACTION ANALYSIS

The samples were prepared as thin layers on slides, and the characteristic diffraction peaks and crystallographic indices of the physical phases of the samples were measured at a rate of 2°/min at 5-80°(2θ) using an XRD-6000 diffractometer from Shimadzu, Japan, equipped with a Cu target for Kα radiation and an acceleration voltage of 30 kV.

$$2d \sin \theta = n\lambda$$

Among them d is the diffraction surface spacing of the sample, θ is the diffraction angle size, n is a non-negative constant, and λ is the wavelength value of X-ray diffraction.

2.1.2. FOURIER TRANSFORM INFRARED SPECTRAL ANALYSIS

The structure of the prepared samples was tested with a Fourier transform infrared spectrometer (FT-IR) model NICOLET 380 from Thermo Scientific, USA. An appropriate amount of powder specimen was mixed and ground well with KBr background material and placed in a mold for compression before testing (the sample was in the form of a thin film). The peaks were also observed at a resolution of 4 cm⁻¹ covering the range of 400-4000 cm⁻¹.

2.1.3. MICROMORPHOLOGICAL ANALYSIS

To study materials, we must study their morphology, and in order to clearly understand the morphology of materials, we usually use high-resolution transmission electron microscopes and scanning electron microscopes. Through these instruments, we can obtain photos up to the nanometer level, both of which can capture the internal structure of the material very clearly.

2.1.4. RAMAN SPECTRAL ANALYSIS

Raman spectrum is a kind of scattering spectrum, which is established according to the scattering phenomenon of light by substances. Different substances have different characteristic spectra, which can be qualitatively analyzed by Raman spectroscopy. Raman scattering does not require a change in dipole moment, but requires a change

in polarization rate, unlike infrared spectroscopy, and it is by taking advantage of the difference between them that the two spectra can complement each other.

2.2. ELECTROCHEMICAL PERFORMANCE TESTING

2.2.1. CYCLIC VOLTAMMETRY (CV)

The CV method is performed by setting constants such as scan voltage window, scan rate and number of scans, and the electrochemical workstation scans the treated material with a triangular waveform of the relevant constants. The current-voltage curve is then obtained, and by analyzing it, the specific capacitance, redox peak intensity and position of the material can be obtained.

2.2.2. CONSTANT CURRENT CHARGE/DISCHARGE METHOD (GCD)

By setting the voltage window, the number of charging and discharging sections, current density level and other test information, the electrochemical workstation uses relevant parameters to charge and discharge the test materials. Then a triangular-shaped GCD diagram is obtained, which can be used to calculate and analyze the properties of the electrode material such as capacitance value and charge/discharge stability. The three-electrode-specific capacitance is calculated by the following equation.

$$C = \frac{I\Delta t}{m\Delta U} \quad (2)$$

Among them C is the specific capacitance of a single electrode, I is the charge/discharge current, Δt is the discharge time, m is the mass of the sample in a single electrode, and Δu is the change in voltage during the charge/discharge time.

2.2.3. ELECTROMAGNETIC WAVE ABSORPTION PERFORMANCE TEST

Paraffin-based mixtures are widely used in laboratory testing of electromagnetic wave absorption properties. In the test, the samples are first mixed well with paraffin wax in various mass ratios. Then, the mixed paraffin-based composites were pressed into circular samples with an inner diameter of 3.04 mm, an outer diameter of 7 mm, and a thickness range of 1.80 to 2.20 mm. The electromagnetic parameters consisted of complex permittivity and complex permeability, and a series of electromagnetic parameters were measured by a vector network analyzer in the frequency range of 2-18 GHz. The coaxial transmission reflection method was chosen to study the samples because of its advantages of small sample size (about 0.01-0.09 g) and wide

test frequency range. The electromagnetic wave absorption characteristics of a material are highly correlated with its own complex permittivity and complex permeability, among them the real part represents the storage capacity of electrical and magnetic energy, and the imaginary part represents the loss capacity of electrical and magnetic energy.

2.3. CHARGING AND DISCHARGING DEVICE SYSTEM DESIGN

Charging and discharging device directly determines the comprehensive performance of the charging and discharging device system, and plays a very important role in the charging and discharging device system. There are two main technical indicators of charging and discharging equipment: one is to have higher performance indicators. Such as reliability, voltage and current stabilization accuracy, speed and pulsation coefficient of dynamic response, voltage and current stabilization accuracy, speed and pulsation coefficient of dynamic response. The second is a more complete self-test function, a high degree of intelligence and control, and the selection of the best parameters for charging and discharging is flexible to improve the capacity and the service life of the device.

The whole system consists of charging and discharging devices such as batteries, DC/DC converters, rectifiers, transformers and control systems. The transformer is connected to the grid on one side and the rectifier on the other side. the DC/DC converter and rectifier are controlled by the control system, which also controls some auxiliary equipment in the system, such as the monitor, power supply and fan.

2.4. FACTORS AFFECTING THE LIFE OF CHARGING AND DISCHARGING DEVICES

In some practical engineering applications, pulse charging and discharging technology basically need to operate at a certain repetition frequency. Under the repetitive charging and discharging conditions of the charging and discharging device, the internal electrodynamic damage and energy loss will be large, which will cause the device life to be reduced or even breakdown. Therefore, it is important to study the charge/discharge life of charge/discharge devices at repetitive frequency to manufacture high-performance, long-life charge/discharge devices and to promote the development of pulse power technology. At the same time, among the many performance parameters of charging and discharging devices, the charging and discharging life is also the most concerned index of some universities, research institutes and equipment manufacturers. When the high voltage pulse charging and discharging device is charged and discharged, its lifetime characteristics are affected by the following factors.

2.4.1. CHARGING VOLTAGE

The life of a charging and discharging device is inversely related to the loss of electric capacity, while the loss of electric capacity is directly related to the working voltage of the charging and discharging device, the relationship between the life of a charging and discharging device and voltage can be expressed as:

$$\frac{L}{L_0} \propto \left(\frac{U}{U_0} \right)^{-m} \quad (3)$$

Among them L , L_0 is the lifetime when the operating voltage of the charging and discharging device is U , U_0 , respectively, and m is the voltage acceleration factor.

2.4.2. ANTI-PEAK VOLTAGE

When the charging and discharging device is subjected to reverse peak voltage below 20%, the impact on its life is not obvious, when the reverse peak voltage reaches 50% or more, the capacity of the charging and discharging device will drop sharply. In the charge/discharge test of the charging/discharging device, the capacity loss caused by the reverse voltage during the test should be considered. When the charging and discharging device is subjected to reverse voltage, the voltage is superimposed on its internal slow polarization electric field, so that the internal medium is subjected to a higher electric field, which accelerates the deterioration of the medium, increases self-healing and reduces the life of the device. The relationship between charging and discharging device life and reverse voltage can be expressed as:

$$\frac{L}{L_0} \propto \left[\frac{\ln(1/\beta)}{\ln(1/\beta_0)} \right]^{-b} \quad (4)$$

Among them β, β_0 are the inverse peak coefficients, L, L_0 correspond to the lifetime when the voltage inverse peak coefficient is β, β_0 respectively, and b is the coefficient.

2.4.3. PEAK DISCHARGE CURRENT

Charging and discharging devices in the process of discharge generated by the pulse of high current will be in its internal electrodes between the formation of a large electrodynamic force. The device in the discharge process at its end of the gold spray flow through the current is the largest, a large electrodynamic force will make the spray gold damage, or even off. When the device is damaged inside the sprayed gold, its internal equivalent series impedance will increase. At this time, a high pulse current will generate high heat in the device, causing it to heat seriously, resulting in the

deterioration of thin film dielectric, the reduction of breakdown field strength, the increase of self-healing and the decline of service life.

2.4.4. TEMPERATURE

When the ambient temperature is 20°C~40°C, the effect of temperature on the life of the charging and discharging device is very small. When the temperature is 40°C~65°C, the life of the charging and discharging device will be reduced by half for every 8°C increase. And when the temperature is above 65°C, the life of the device decreases sharply. Therefore, when conducting charge/discharge tests on the charging/discharging device, the influence of ambient temperature and the internal working temperature of the device on its life must be considered. The relationship between the life of the charging and discharging device and the temperature is as follows.

$$L \propto e^{-\gamma T} \quad (5)$$

Among them T is the operating temperature of the charging and discharging device, which is the sum of the ambient temperature and the temperature rise of the internal medium. L is the life of the charging and discharging device at temperature T , and γ is the material property index, which depends on the internal medium material.

2.4.5. OTHER FACTORS

This includes the number of charge/discharge cycles, charge/discharge frequency, charge voltage hold time, and first past zero time of capacitance-voltage are closely related to the lifetime characteristics of the charge/discharge device.

In this section, the methods of structural characterization of functional materials and the test methods of charge/discharge characteristics are elaborated. Then we describe the design of the entire high-voltage pulse charge/discharge device system and enumerate the devices involved in the system. Then we discuss and analyze the factors affecting the device life due to the frequent charging and discharging characteristics of the charging and discharging device, and lay the theoretical foundation for the subsequent discussion.

3. RESULTS AND DISCUSSION

The use method of the charging and discharging device is to first close the circuit breaker at the input end of the device and energize the whole device. The control program of the device starts to run, and checks the status of all parts of the device, including whether the cabinet door of the device is closed, whether the emergency stop switch is triggered, etc. If there is an error condition, the device's fault signal light will illuminate and the operator interface will have an error indication. If the system

status is normal, the battery will be connected to the plug box of the charging and discharging device through the navigation plug. If the connection line is reliably connected, the standby signal light on the corresponding plug box and the standby signal light of the device will be on, otherwise, please check the connection line and reconnect. At this time, the control system will detect the battery voltage at the system output and display the battery power information on the device. If the battery voltage is too low or the connection cable is disconnected during the charging and discharging process, the system will enter the fault handling process.

3.1. CHARGING PROCESS

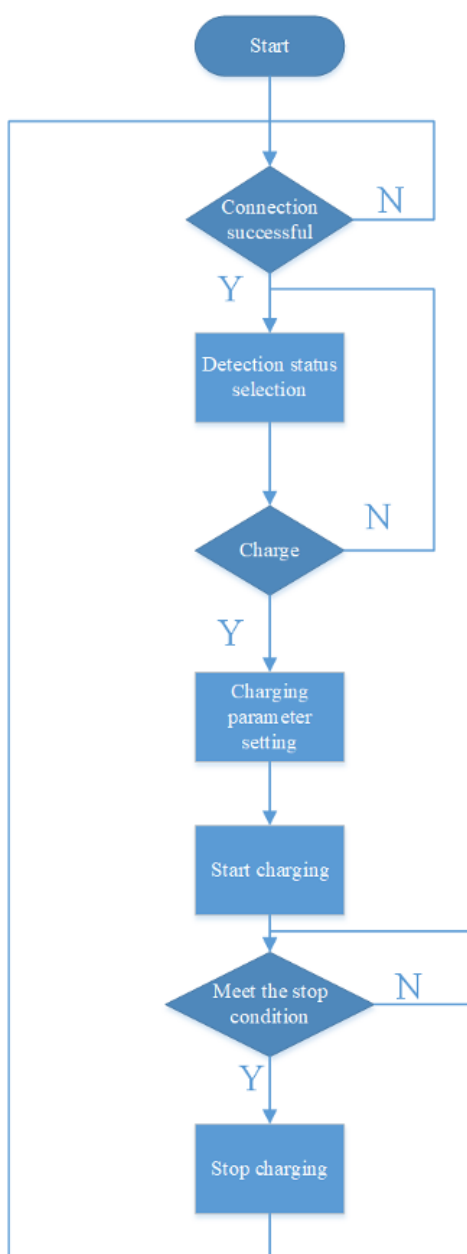


Figure 1. Charging flow chart

The charging control flow chart is shown in Figure 1. When the knob of the plug-in box selects charging, the device will jump to the setting interface of charging

parameters, which can select the system default parameters or set the parameters manually. Selecting the system default parameters, the control system will control the charging module to charge according to the default command value, charging the battery at 150A in constant current and voltage limiting mode, and switching to constant voltage and current limiting mode when the battery voltage reaches 120V until the end of charging. Select manual setting parameters to set the constant current limit charging current value, constant current limit charging voltage value and charging time for lead-acid batteries, and stop charging when the battery is fully charged in constant current limit mode or when the charging time is over.

After setting the parameters, click the start button on the device interface to start charging. The control system of the device will send the parameter setting command to the charging module, and send the start command after the charging module returns the parameter confirmation information, and the charging module receives the start command and then opens the drive to start running.

When the equipment is running, the actual charging current, charging voltage, charging time, battery voltage, power state and other parameters can be observed on the operation interface, and there is a stop charging button to control the work of the charging module. During operation, the control system of the device will keep sending parameter query commands to the charging module via CAN communication and update the new data acquired into the device. At the same time, it will judge whether the charging module is normal or not based on the operating status of the feedback charging module, and if there is any abnormality it will stop charging and enter the fault handling process.

If there is no abnormality in the charging process of the device, when the charging end condition is met, the control system of the device will send a stop command to the charging module, and the charging module will stop the operation of the charging module after receiving the command. The operation interface will remind the user that the charging process is finished and please unplug the connection cable. During the whole charging process, the control system will also send the status and operation parameters of the whole device to the remote background, which is convenient for remote monitoring of the device.

3.2. DISCHARGE PROCESS

Figure 2 shows the discharge control flow chart of the charging and discharging devices. When entering the discharge mode, the operation interface will enter the discharge mode, in which the default parameters can be used to monitor and control the discharge process. You can also customize the control parameters according to your needs to achieve personalized control of the discharge process. When the default parameters are used, the control system will control the discharge module to discharge according to the default current command value of 80A. When the battery voltage is lower than 65V, the discharge will stop and the discharge time will be

recorded to judge the battery life status. Select the manual setting parameter to set the discharge current and discharge time of the lead-acid battery, and stop the discharge when the battery voltage is lower than 65V or when the discharge time is over. After setting the operating parameters, click Run in the operation interface. During the discharge process, the current, voltage, running time of each work step and other parameters can be displayed on the screen, so that users can easily observe the discharge status. It is also possible to control the work of the charging module through this operation interface. The control system of the device will keep sending parameter query commands to the charging module through CAN communication during the operation process and update the new data obtained to the device.

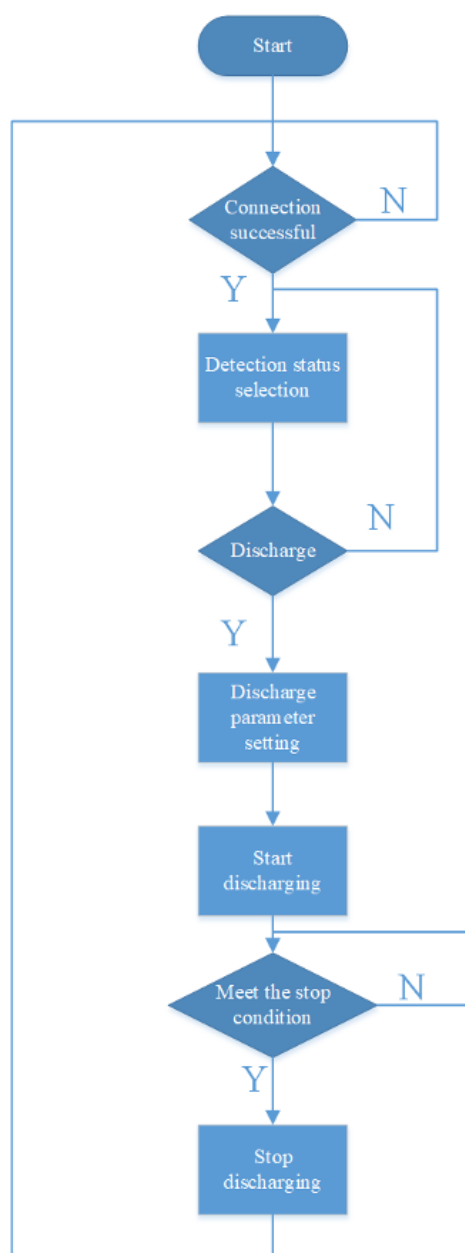


Figure 2. Discharge flow chart

3.3. VERIFICATION OF CHARGING AND DISCHARGING FUNCTIONS

During the operation of the charging module of the device, when the user changes the setting value of the charging output current through the control device, the charging module should be able to respond quickly by adjusting the output current to the new commanded value. In this test, the charging module was adjusted from a steady-state output of 145A to a steady-state output of 75A in a dynamic process, and its output current dynamic regulation curve is shown in Figure 3.

As can be seen from Figure 3, the time required to regulate the charging module output current from steady-state output 160A to steady-state output 90A is 22ms under the design condition, and during the actual test, the regulation time of the charging module output current from steady-state output 145A to steady-state output 75A is only 20ms, which is 2ms less than the design condition. This is due to the fact that the DC/DC part of the charging module is operating in constant current and voltage-limiting mode. The maximum value of the output of the PI controller of the voltage outer loop is set to the value of the constant current limit charging current. When the charging module works in constant current limit mode, the voltage of the battery is lower than the constant current limit charging voltage, the PI controller of the outer voltage loop will be saturated and the output value is the constant current limit charging current value. At this time, the DC/DC part of the controller is equivalent to only the current inner loop single loop working. When the charging process transitions to the constant voltage current limiting mode, the outer voltage loop of the controller returns to the adjustable area and controls the output current of the module together with the inner current loop. Therefore, the charging and discharging device has good current dynamic regulation during the charging process.

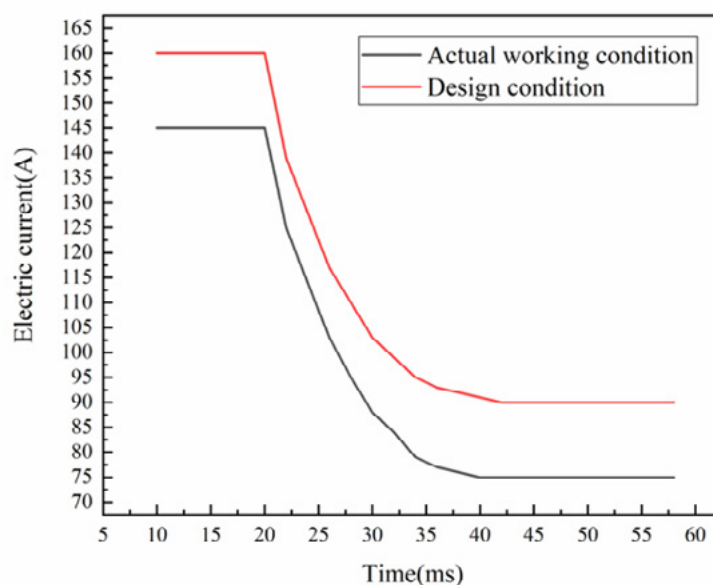


Figure 3. Charging state output current dynamic regulation curve

3.4. DYNAMIC ADJUSTMENT OF THE INPUT CURRENT OF THE DISCHARGE MODULE

The dynamic adjustment of the discharge state input current is shown in Figure 4. When the user changes the set value of the discharge input current through the device during the operation of the discharge module of the device, the discharge module should be able to respond quickly by adjusting the input current to the new commanded value. Here, the dynamic process of adjusting the discharge module from a steady-state input of 60 A to a steady-state input of 40 A at an input voltage of 96 V is measured, and the response time of the discharge module is about 0.14 s. This is due to the introduction of a negative feedback link in the circuit, and the discharge circuit is a typical nonlinear system that cannot be parameterized with feedback links using methods such as frequency domain analysis of self-control theory. However, when the circuit is at a certain steady-state operating point, there is a linear relationship between the small disturbances of the state variables in the circuit. Therefore, the system has good performance in the dynamic regulation of the input current of the discharge module.

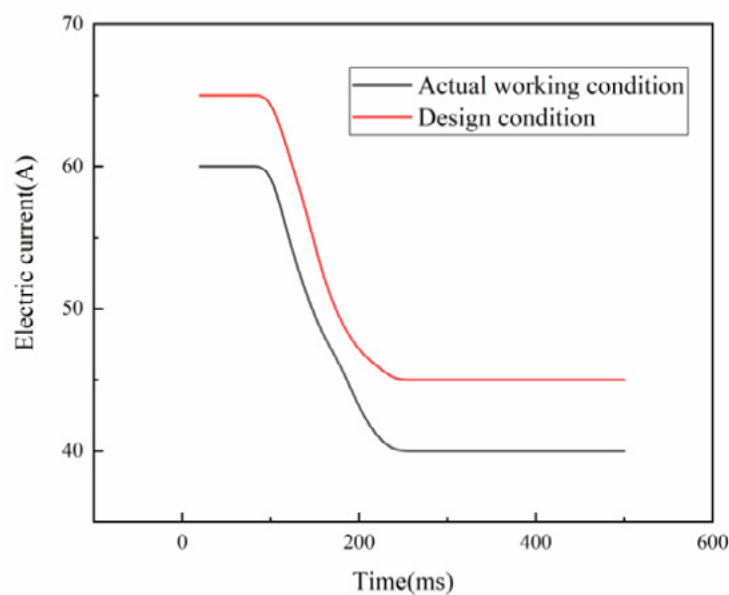


Figure 4. Discharge state input current dynamic regulation

In summary, this section firstly designs the charging and discharging process of this charging and discharging system, and tests the dynamic regulation performance of the charging module output current and the dynamic regulation performance of the discharging module input current for this functional material-based high-voltage electric pulse charging and discharging device.

4. CONCLUSION

Based on the new functional materials, a new high-voltage electric pulse charging and discharging device is developed in this paper. The charging and discharging control process is designed in detail, and the dynamic regulation performance of the output current of the charging module and the input current of the discharging module is tested and verified. The specific research results are as follows.

1. Based on the technical specifications of charging and discharging the device, the topology of the discharging module was selected as a modified Buck circuit. The charging module uses a two-stage circuit topology of VIENNA rectifier plus a phase-shifted full bridge converter. The device is described at the system level and the workflow of each function of the device, such as the charging process and discharging process, is designed.
2. Through the dynamic adjustment of the charging module output current, during the test, the charging module output current is adjusted from steady-state output 145A to steady-state output 75A, and the adjustment time is only 20ms. therefore, the charging and discharging equipment has good current dynamic adjustment ability in the charging process.
3. In the dynamic adjustment test of the input current of the discharge module, the input voltage is 96V, and the dynamic process of adjusting the discharge module from steady-state input 60A to steady-state input 40A is measured, and the response time of the discharge module is about 0.14s. Therefore, the system has good performance in the dynamic adjustment of the input current of the discharge module.

In this paper, the input filter circuit is added in the front of the buck circuit, and the resonant peak is introduced into the Bode diagram of the discharge system, which is easy to causes the instability of the discharge system. In this paper, the method of reducing the amplitude-frequency gain of the system is adopted, so that the amplitude gain at the resonant frequency is less than 0, and the discharge system is stable, but the crossing frequency of the system is small, and the response time of the system is long. Therefore, the RC branch can be connected in parallel with the input filter capacitor in the future. When the capacitance C should be much larger than the value of the filter capacitance C₁, the specific impact and effect of this method can be studied.

REFERENCES

- (1) Yuan, Z. (2020). Research on Environmental Cost Management Problems and Countermeasures of China's Iron and Steel Enterprises. *International Journal of Social Science and Education Research*, 3(5), 159-162.

- (2) Cao, M., Hu, Y., & Cheng, W. (2022). Lignin-based multi-scale cellular aerogels assembled from co-electrospun nanofibers for oil/water separation and energy storage. *Chemical Engineering Journal*, 436.
- (3) Xiao-Lei, M. A., Meng, J. S., Dan-Ping, F. U. (2020). Study on environmental geological problems and prevention countermeasures of typical ecologically vulnerable areas—Take the Bashang area in Hebei as an example. *Ground Water*.
- (4) Ansari, A. S., Kim, H., Ahmed, A. T. A., & Im, H. (2022). Ion-exchange synthesis of microporous Co_3S_4 for enhanced electrochemical energy storage. *International Journal of Energy Research*, 46(4), 5315-5329.
- (5) Yi, T., Jin, C., Hong, J., & Liu, Y. (2022). Layout analysis of compressed air and hydraulic energy storage systems for vehicles. *Advances in Mechanical Engineering*.
- (6) Wang, B., & Lin, P. (2022). Whether China's overseas energy infrastructure projects dirtier or cleaner after the Belt and Road Initiative?. *Energy Policy*, 166.
- (7) Yu, K., Li, B., Zhang, H., Wang, Z., & Pan, J. (2021). Critical role of nanocomposites at air–water interface: from aqueous foams to foam-based lightweight functional materials. *Chemical Engineering Journal*, 416, 129121.
- (8) Lee, D. (2021). Functional material developments of fuel cells and the key factors for real commercialization of next-generation energy devices. In *Sustainable Materials for Next Generation Energy Devices*.
- (9) Chai, Y., Chen, A., Bai, M., Peng, L., Shao, J., & Yuan, J., et al. (2022). Valorization of heavy metal contaminated biomass: recycling and expanding to functional materials. *Journal of Cleaner Production*.
- (10) Zeng, H., & Huang, F. (2022). Energy materials in the new era. *Journal of Inorganic Materials*, 37(2), 113-116.
- (11) Lin, Z., Li, S., & Huang, J. (2021). Natural cellulose substance-based energy materials. *Chemistry - An Asian Journal*.
- (12) Lu, N., Zhuo, Z., Guo, H., et al. (2018). A New Two-Dimensional Functional Material with Desirable Bandgap and Ultrahigh Carrier Mobility. *Journal of Physical Chemistry Letters*.
- (13) Xiao, T., Zhao, L., Ge, H., et al. (2022). Cobalt oxyhydroxide decorating hollow carbon sphere: A high-efficiency multi-functional material for Li-S batteries and alkaline electrocatalysis. *Chemical Engineering Journal*, 439, 135790.
- (14) Li, D., Zhang, H., Sun, Y. (2021). A CO₂ gas thermal conductivity sensor based on GO/ α -Al₂O₃ functional material. *IEEE Sensors Journal*, (99), 1-1.
- (15) Wang, X., Li, S., Cheng, T., et al. (2022). Overview of photonic devices based on functional material-integrated photonic crystal fibers. *Journal of Physics D: Applied Physics*, 55(27), 273001.
- (16) Compagnone, D. (2021). Graphene Nanoflakes Incorporating Natural Phytochemicals Containing Catechols as Functional Material for Sensors. *Chemistry Proceedings*, 5.
- (17) Ma, Y., Chen, N., & Lv, H. (2021). Back propagation mathematical model for stock price prediction. *Applied Mathematics and Nonlinear Sciences*. doi:10.2478/AMNS.2021.2.00144.

- (18) Rui, J., Guan, R., Zhang, J., et al. (2021). Design of Information Acquisition System for High Voltage Pulse Power Supply. *Journal of Physics: Conference Series*, 1894(1), 012094.
- (19) Yilmaz, M. S., Sahin, O. (2018). Applying high voltage cathodic pulse with various pulse durations on aluminium via micro-arc oxidation (MAO). *Surface and Coatings Technology*, S0257897218304614.
- (20) Rao, P., Ouyang, P., Nimbalkar, S., et al. (2022). Mechanism Analysis of Rock Failure Process under High-Voltage Electropulse: Analytical Solution and Simulation. *Materials*, 15.
- (21) Dong, B., Zhao, X., Zhang, Y., et al. (2019). Study on parameter optimization of bipolar high-voltage pulse dielectric barrier discharge denitrification experiment. *Environmental Pollution & Control*.
- (22) Li, C., Wang, X., Duan, L., et al. (2022). Study on a Discharge Circuit Prediction Model of High-Voltage Electro-Pulse Boring Based on Bayesian Fusion. *Energies*, 15.
- (23) Li, Y., He, M., Shi, F. (2021). High voltage pulse-enabled coal desulfurization and deashing – Part 1: Selective breakdown of mineral matter. *Fuel*, 300, 120970.
- (24) Bx, A., Xiang, W. A., Wow, B. (2021). Process control of charging and discharging of magnetically suspended flywheel energy storage system. *Journal of Energy Storage*.
- (25) Folayan, T. O., Dhindsa, K., Atienza, D., et al. (2022). Direct Recycling of Cathode Active Materials from EV Li-Ion Batteries. IOP Publishing Ltd.
- (26) Jiaying, L. I., Chen, J., Zhang, X. (2018). Coordinated Control of Charging and Discharging for EV-sharing. *Proceedings of the CSU-EPSA*.
- (27) Feng, S., Li, T. H., Liao, Z. X. (2019). Research and Implementation of Charging and Discharging Device Based on DSP Bi-directional DC-DC Converter. DEStech Publications.
- (28) Guo, L. N., Gao, Z. L., Wang, L. L., et al. (2018). Design of Control System for Automatic Charging and Discharging Device of Oxygen Sensor Gasket. *Instrument Technique and Sensor*.
- (29) Wang, Z., Huang, W., Tong, L., et al. (2020). Design of Timing Charging and Discharging System for Pneumatic or Hydraulic Pressure Device Based on STM32. In *EITCE 2020: 2020 4th International Conference on Electronic Information Technology and Computer Engineering*.
- (30) Sodhi, G. S., Jaiswal, A. K., Vigneshwaran, K., et al. (2019). Investigation of charging and discharging characteristics of a horizontal conical shell and tube latent thermal energy storage device. *Energy Conversion and Management*, 188(MAY), 381-397.
- (31) Kim, J., Joonhyoung, et al. (2019). A Proposed Fast Charging and High-Power System for Wireless Railway Trains Adopting the Input Voltage Sharing Topology and the Balancing Control Scheme. *IEEE Transactions on Industrial Electronics*, 67(8), 6407-6417.
- (32) Choi, G. H., Yang, J. H., Jeong, T. Y., et al. (2018). Charging and Discharging Characteristics Analysis of a Battery for a Hybrid Electric Propulsion System. *Journal of Power System Engineering*, 22(4), 39-46.